Title

Neutrophil Granulopoiesis Optimized Through Ex Vivo Expansion of Hematopoietic Progenitors in Engineered 3D Gelatin Methacrylate Hydrogels

Journal

Advanced Healthcare Materials, 13(14)

ISSN

2192-2640

Authors

Cirves, Evan

Vargas, Alex

Wheeler, Erika E

et al.

Publication Date

2024-06-01

DOI

10.1002/adhm.202301966

Peer reviewed

ADVANCED HEALTHCARE MATERIALS
www.advhealthmat.de

Neutrophil Granulopoiesis Optimized Through Ex Vivo Expansion of Hematopoietic Progenitors in Engineered 3D Gelatin Methacrylate Hydrogels

Evan Cirves, Alex Vargas, Erika E. Wheeler, Jonathan Kent Leach, Scott I. Simon, and Tomas Gonzalez-Fernandez**

Neutrophils are the first line of defense of the innate immune system. In response to methicillin-resistant Staphylococcus aureus infection in the skin, hematopoietic stem, and progenitor cells (HSPCs) traffic to wounds and undergo extramedullary granulopoiesis, producing neutrophils necessary to resolve the infection. This prompted the engineering of a gelatin methacrylate (GelMA) hydrogel that encapsulates HSPCs within a matrix amenable to subcutaneous delivery. The authors study the influence of hydrogel mechanical properties to produce an artificial niche for granulocyte-monocyte progenitors (GMPs) to efficiently expand into functional neutrophils that can populate infected tissue. Lin-cKIT+ HSPCs, harvested from fluorescent neutrophil reporter mice, are encapsulated in GelMA hydrogels of varying polymer concentration and UV-crosslinked to produce HSPC-laden gels of specific stiffness and mesh sizes. Softer 5% GelMA gels yield the most viable progenitors and effective cell-matrix interactions. Compared to suspension culture, 5% GelMA results in a twofold expansion of mature neutrophils that retain antimicrobial functions including degranulation, phagocytosis, and ROS production. When implanted dermally in C57BL/6J mice, luciferase-expressing neutrophils expanded in GelMA hydrogels are visualized at the site of implantation for over 5 days. They demonstrate the potential of GelMA hydrogels for delivering HSPCs directly to the site of skin infection to promote local granulopoiesis.

1. Introduction

Polymorphonuclear leukocytes (PMNs), commonly known as neutrophils, are the most abundant white blood cells in circulation and are crucial in the innate immune response against pathogens.[1,2] They are the first line of defense in combating skin infection and are necessary for removing bacteria and initiating the process of tissue healing. PMNs are continuously produced by hematopoietic stem and progenitor cells (HSPCs) in the bone marrow and released into the circulation to surveil tissue. In the event of a dermal wound and acute infection, HSPCs migrate out of their niche in the bone marrow and undergo emergency granulopoiesis which increases PMN production and their availability within circulation.[3,4] Human patient populations that suffer from acute neutropenia, such as those receiving chemotherapy treatment for acute myeloid leukemia (AML) are depleted of HSPCs and are prone to develop severe, sometimes fatal, infections.[5] These patients are typically infused with donor leukocytes, but such treatments require multiple infusions with an increased probability of systematic reinfection.[6] Ex vivo produced PMNs derived from HSPC cultures represent a potential source of autologous cells for infusion or delivery to sites of infection.[7] This approach, however, has not been used clinically due to the high cost and inefficient expansion of CD34+ HSPCs in suspension cultures within a bioreactor and the lack of criteria for determining the potency of myeloid expansion for

E. Cirves, A. Vargas, E. E. Wheeler
Department of Biomedical Engineering
University of California at Davis
451 East Health Sciences Drive, 2303 GBSF, Davis, CA 95616, USA

The ORCID identification number(s) for the author(s) of this article can be found under https://doi.org/10.1002/adhm.202301966

DOI: 10.1002/adhm.202301966

E. E. Wheeler, J. K. Leach
Department of Orthopaedic Surgery
UC Davis Health
4860 Y Street, Suite 3800, Sacramento, CA 95817, USA

S. I. Simon
Department of Biomedical Engineering and Dermatology
University of California at Davis
Davis, CA 95616, USA
E-mail: sisimon@ucdavis.edu

T. Gonzalez-Fernandez
Department of Bioengineering
Lehigh University
124 E Morton Street, Health Science and Technology Building,
Bethlehem, PA 18015, USA
E-mail: tomasgf@lehigh.edu

any given donor HSPCs.[8] Furthermore, bolus injection of purified allogeneic or donor PMNs directly into chronic wounds results in a high rate of cell apoptosis and ineffective antibacterial function that limits the therapeutic efficacy of infusion.[9–12]

In addition to emergency granulopoiesis, which produces PMNs within the bone marrow, HSPCs can extravasate into the circulation and migrate into infected wounds where they proliferate and differentiate locally into mature PMNs following toll-like receptor 2 (TLR2) mediated recognition of *Staphylococcus aureus* (*S. aureus*).[13,14] Local granulopoiesis accounts for up to 30% of PMNs in a dermal site of infection, making them crucial for survival in a mouse model of methicillin-resistant *S. aureus* (MRSA) infection.[13] Specifically, inducing an acute *S. aureus* infection in a full-thickness skin wound resulted in a twofold increase in PMNs in circulation and a tenfold increase in PMN recruitment to the infected wound.[13] In fact, HSPC trafficking and local myeloid granulopoiesis at the site of MRSA infection is a critical host immune tactic for circumvention of impaired PMN recruitment mediated by the virulence factor alpha-toxin.[15] This discovery motivates the development of local HSPC administration as an immune therapy to combat intractable infections in patients with impaired PMN tissue recruitment or insufficient vascular perfusion and antibacterial function, such as observed in diabetic wounds.[16] One challenge to overcome in exploiting local granulopoiesis is the design of a bone marrow mimetic niche that facilitates cell-matrix and cell-cell signaling via paracrine growth factors (e.g., stem cell factor (SCF), granulocyte colony-stimulating factor (G-CSF), FMS-like tyrosine kinase 3 (Flt3)) and interleukins that promote effective terminal PMN differentiation of CD34+ HSPCs.

A limitation of engineered cell therapies is the vehicle used for delivery since bolus injection can lead to cell apoptosis and low therapeutic efficacy. Thus, a strategy to encapsulate HSPCs in a hydrogel-based biomimetic matrix can provide for the maintenance of myeloid progenitors and sustained and localized release of PMNs within the site of inflammation. HSPCs and other stem-like progenitor populations are preserved longer within collagen hydrogels versus suspension cultures, which is especially critical in the case of granulopoiesis that requires maintenance of the self-renewal properties of HSPCs.[17] Furthermore, the tuning of biochemical properties of a substrate can dictate the extent of HSPC function by adjusting the substrate's storage modulus and porosity to mimic the in vivo bone marrow environment that preserves stem-like populations. For example, previous studies focusing on the co-culture of HSPCs and mesenchymal stem cells (MSCs) in gelatin methacrylate (GelMA) resulted in the production of lineage-positive (Lin+) PMN progenitors while maintaining stem populations.[18] However, these studies did not quantify the efficiency of PMN expansion or maturation into functional phagocytes.[18]

In the current study, we produced GelMA hydrogels with prescribed stiffness to simulate the bone marrow niche with the objective of optimizing the efficiency of HSPC granulopoiesis and local generation of functional PMNs. We compared the functional phenotype of PMNs within the hydrogels with those grown in suspension to define their capacity for function in both in vitro and in vivo mouse studies. We also leveraged the previously established C57BL/6 mouse lines including enhanced green fluorescent protein–lysozyme M (EGFP-LysM) expressing mice and MRP8-FFLUC transgenic mice for quantitation of myeloid differentiation and expansion.[19] This enabled us to establish the potential of this approach for in vivo delivery of functional PMNs.

2. Results

2.1. GelMA Hydrogel Mechanical Properties Determine HSPC Survival and Cell-Matrix Interactions

During emergency granulopoiesis, de novo expansion of PMNs by HSPC progenitors occurs in the bone marrow which provides a rapid increase in the number of mature PMNs released into circulation to meet the demand for recruitment at sites of infection. To mimic the mechanical properties of the perivascular endosteal regions where HSPCs undergo granulopoiesis, we cultured HSPCs in GelMA over a range in stiffness.[20] Three GelMA concentrations (5%, 10%, and 20%) were selected to produce gels with Young's moduli ranging from 0.25 to 24.7 kPa. While 5% GelMA produced hydrogels with the lowest storage modulus (**Figure 1**A), they also exhibited the highest swelling ratio and porosity in comparison to 10% and 20% (Figure 1B,C). To explore the effects of the physical properties of the hydrogels on cell survival, HSPCs were encapsulated in GelMA and maintained in culture. Following 1 day of encapsulation, we observed greater DNA content for cells in 5% GelMA gels compared to cells in 10% and 20% gels (Figure 1D). We evaluated the relationship between DNA content and cell apoptosis by assessing caspase 3/7 activity, which revealed higher apoptosis as the density of GelMA increased (Figure 1E). In addition to DNA and caspase 3/7 activity, live/dead staining confirmed a higher frequency of cell mortality in the 10% and 20% GelMA gels in comparison to the 5% gels, in which nearly all cells remained viable (≈95%) (Figure 1F; Figure S1C, Supporting Information). Cell morphology was also evaluated by staining of F-actin cytoskeleton staining. While cells encapsulated in 5% GelMA frequently exhibited a polarized morphology with multiple pseudopods, cells in 10% and 20% GelMA were comparatively smaller and remained spherical (Figure 1G; Figure S1A,B, Supporting Information), suggesting increased cell-matrix interactions in the 5% gels. To confirm that the observed differences were due to GelMA culture and not to UV exposure during GelMA crosslinking, a control experiment was conducted to evaluate the effect of UV treatment on HSPC suspensions after 3 days of culture, revealing no difference in cell viability or oxidative stress (Figure S2, Supporting Information).

2.2. HSPC Culture in GelMA Hydrogels Increases Granulopoiesis and Neutrophil Differentiation in Comparison to Cells Cultured in Suspension

Previous reports have confirmed the key role of hydrogel mechanics in HSPC maintenance and differentiation, but the role of the 3D environment in HSPC granulopoiesis remains unexplored.[18] To evaluate the effects of 3D GelMA culture on HSPC granulopoiesis in comparison to equal numbers seeded in suspension culture, HSPCs isolated from the bone marrow of LysM-EGFP mice were encapsulated in 5% GelMA and maintained in culture for 3 days in myeloid differentiation media supplemented with G-CSF, SCF, IL-3, IL-6, and Flt-3. LysM-EGFP

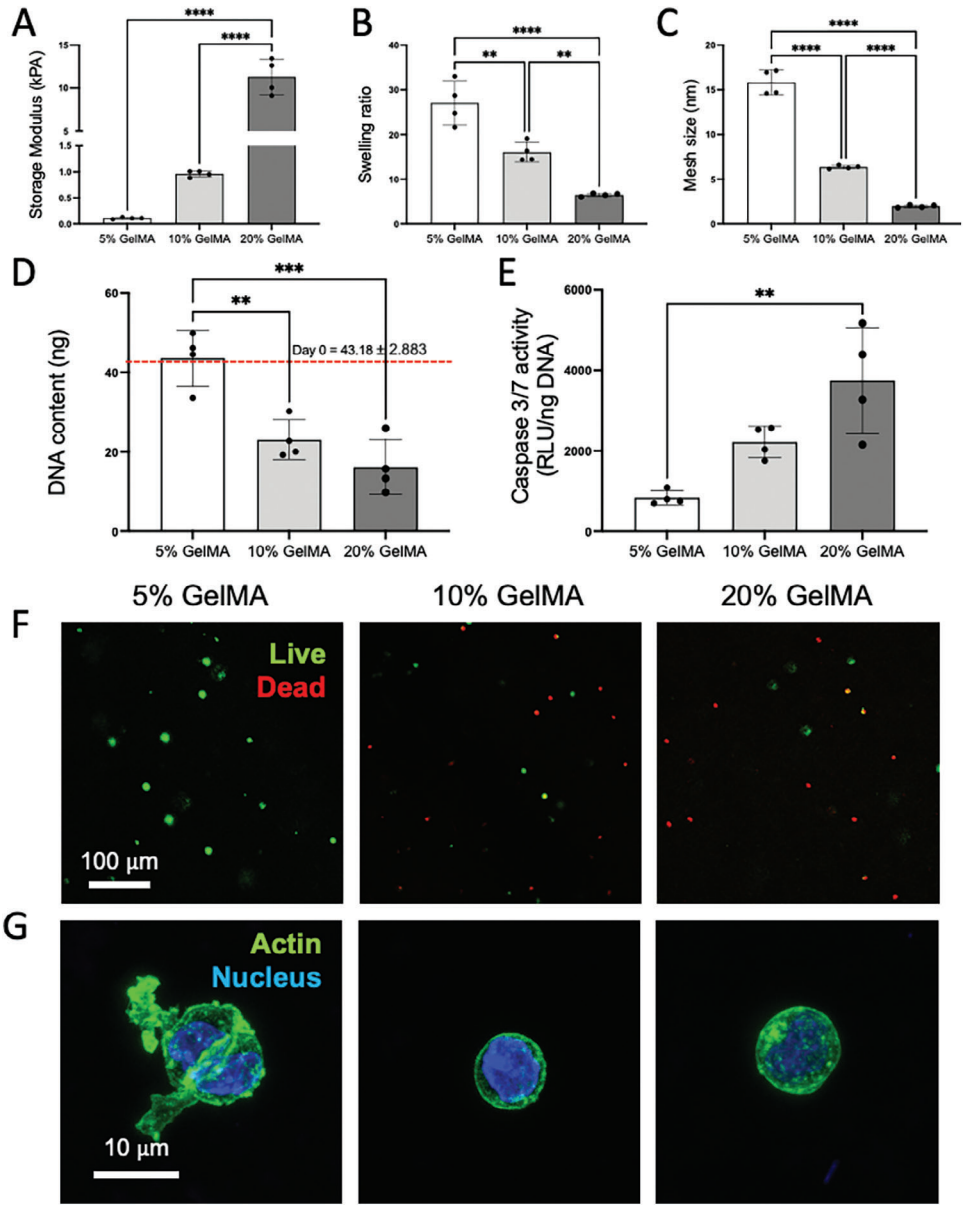

Figure 1. GelMA hydrogel mechanical properties correlate with HSPC survival and a motile morphology. A) Storage modulus, B) swelling ratio, and C) mesh size of either 5%, 10%, or 20% GelMA hydrogels after production (N = 4). D) DNA content and E) caspase 3/7 activity in HSPC-laden GelMA hydrogels 24 h after cell encapsulation (N = 4). F) Live/dead (living cells in green, dead cells in red) characterization of encapsulated HSPCs 24 h after hydrogel production. G) Fluorescent imaging of HSPC actin cytoskeleton in the different GelMA gels 24 h after production. For F and G, representative images out of six, two independent experiments. ** Denotes significance ($p < 0.01$); **** ($p < 0.0001$).

mice possess the enhanced green fluorescent protein (EGFP) inserted in the lysozyme M (LysM) promoter region, thereby facilitating the quantification of mature PMNs that express the highest levels of LysM-EGFP. In addition, HSPC differentiation was assessed by identifying undifferentiated HSPCs (LSK+) and granulocyte-monocyte progenitors (GMPs) that express low levels of LysM-EGFP (**Figure** 2A).[21] After 3 days of in vitro culture, equivalent numbers of viable cells were observed in suspension and GelMA gels (Figure 2B), but there were significantly more GMPs and PMNs detected in dissolved gels (Figure 2B,C). Additionally, we determined that the fold expansion of GMPs and PMNs per HSPC encapsulated in GelMA was significantly higher than in suspension (Figure 2D), although the total fold expansion was similar in both groups (Figure 2E). We conclude there is enhanced differentiation and expansion of PMN derived from HSPC cultured in 3D gels as cultured in suspension.

HSPCs and PMNs express metalloproteases and catabolic enzymes that degrade collagen and other ECM components.[22,23] We hypothesized that this process facilitates the escape of PMNs from their porous 3D GelMA microenvironment where they remain viable in suspension (**Figure** 3A). To analyze the phenotype of cell populations that escaped from the GelMA, HSPCs were

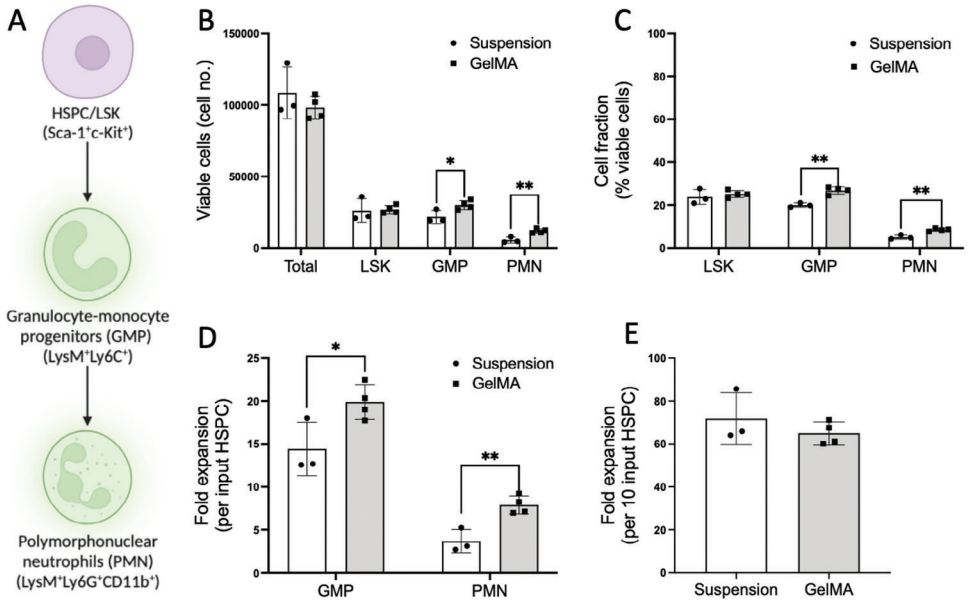

Figure 2. HSPC encapsulation into 5% GelMA hydrogels increases their neutrophil differentiation potential in comparison to suspension culture. A) To assess the expansion potential of HSPCs toward neutrophils, LysM-EGFP cells were stained with Sca-1$^+$c-KIT$^+$ to determine undifferentiated HSPCs (LSK cells), with Ly6C$^+$ to determine granulocyte-monocyte progenitors (GMPs), and with Ly6G$^+$CD11b$^+$ to assess the polymorphonuclear neutrophil populations (PMNs). After 72 h of in vitro culture in either suspension or 5% GelMA gels, cells were isolated, and the B) total number of viable cells was determined through FACS. C) Cell fractions (% of viable cells) for LSK, GMP, and PMN cells were also determined. D) Myeloid expansion per input HSPC toward GMP or PMN phenotypes and E) the total fold expansion of all cells detected per input HSPCs were also determined after the culture time. N = 3 in suspension and 4 in GelMA. Suspension data points are represented with a dot symbol and white bars, and GelMA with a square symbol and light grey bars. * Denotes significance ($p < 0.05$) in comparison to the rest of the groups; ** ($p < 0.01$) in comparison to the rest of the groups.

cultured in either suspension or GelMA for 7 days in differentiation media. We observed that equivalent fractions of viable LSK, GMP, and PMN populations were detected between suspension and GelMA cultured HSPC (Figure 3B). In the GelMA group, ~40% of cells escaped from intact 3D gels (Figure 3C). To further investigate the mechanism of HSPC escape from GelMA gels, matrix metalloprotease (MMP) 8 and 14 gene expression was analyzed at 7 days. Cells encapsulated in GelMA expressed significantly higher levels of MMP14 when compared with those that escaped (Figure S3A, Supporting Information). Since MMP-14 activity is broad-acting collagenous and required for proper neutrophil migration and endothelial transmigration, this data is consistent with the increased capacity of encapsulated cells to degrade the GelMA matrix. In contrast, MMP8 expression exhibited greater variability, and significant differences in expression between encapsulated and escaped cells were not detected (Figure S3B, Supporting Information). While LSK constituted the highest percentage of cells that remained inside the gels (In-GelMA), GMP represented the highest fraction that escaped (Figure 3D). Moreover, the mean fluorescence intensity of LysM-EGFP$^+$ cells was higher in cells remaining in GelMA and those that escaped compared to suspension (Figure 3D). Progenitor expansion within the GelMA gels at day 7 was confirmed by fluorescence imaging of CD117+ progenitors, a fraction of which co-expressed LysM-EGFP (Figure S3C, Supporting Information). Thus, we conclude that LSK cells self-renewed at higher rates resulting in greater expansion of mature PMNs capable of migration out of GelMA compared to suspension-grown cells.

2.3. Neutrophils Originated from GelMA Encapsulated HSPCs Exhibit Equivalent or Higher Levels of Activation and Function in Comparison to Culture in Suspension Conditions

A hallmark of the antimicrobial and inflammatory activity of PMNs is their capacity to produce superoxide radicals, i.e., reactive oxygen species (ROS), due to the NADPH oxidase complex (**Figure** 4A).[24] To assess PMN activation in GelMA versus suspension after 7 days of culture, ROS production was quantified through activation of NADPH-oxidase in response to the addition of the secretagogue phorbol myristate acetate (PMA, 10 ng mL^{-1}) (Figure 4B). As a positive control, PMNs freshly isolated from mouse bone marrow were also assessed. PMNs expanded in GelMA generated equivalent levels of ROS as compared to those produced in suspension both at baseline and with PMA stimulation (Figure 4B). By comparison, naïve PMN isolated from bone marrow exhibited very low baseline levels and lower stimulated ROS production. We conclude that ex vivo PMN expansion in the 3D microenvironment effectively produces mature PMNs that are capable of ROS production at levels on par with those cultured in suspension.

CD11b is upregulated to the plasma membrane in response to degranulating stimuli, where it regulates leukocyte adhesion and extravasation (Figure 4A).[25] To further assess PMN maturation and functionality, we quantified the relative surface expression of CD11b on bone marrow PMNs compared with cells expanded in suspension or GelMA gels. In response to PMA stimulation, cells encapsulated in GelMA or isolated from bone marrow upregulated ≈100% more CD11b compared with

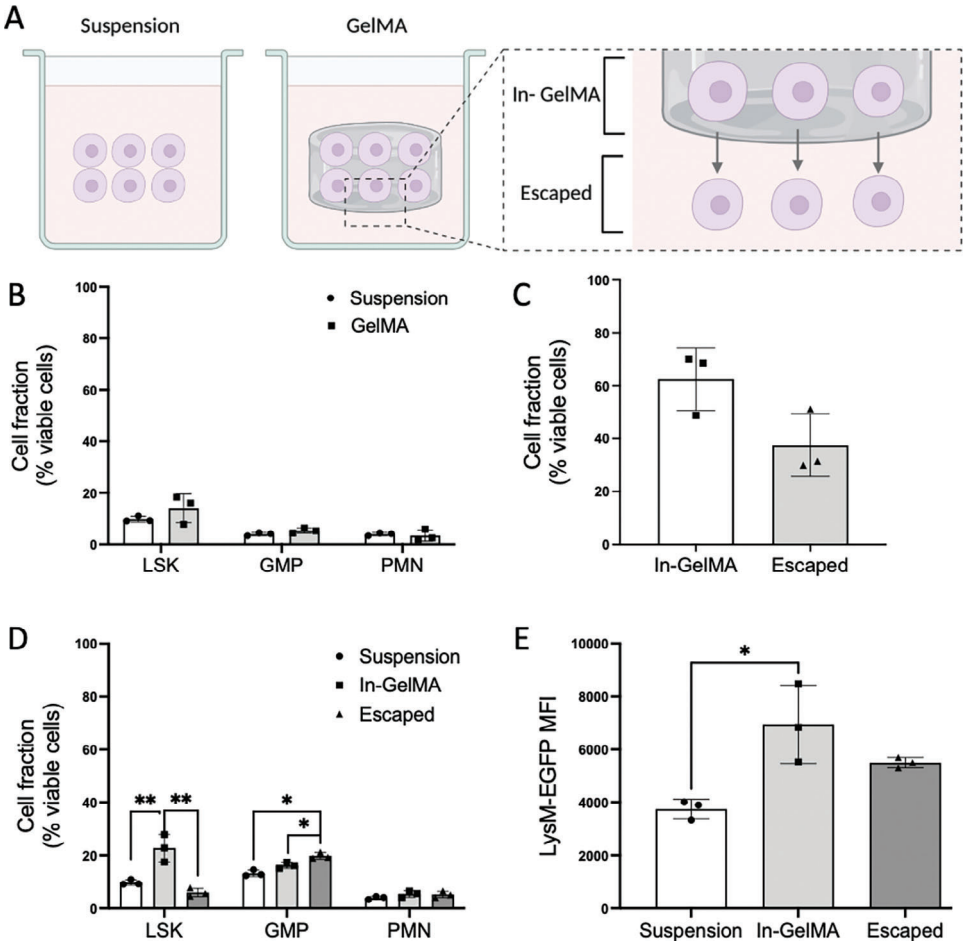

Figure 3. Phenotypic differences between HSPCs that escaped the GelMA hydrogels and cells that remained inside the biomaterial after 7 days of in vitro culture in differentiation conditions. A) Graphical representation of analyzed cell populations defining the cells that remained encapsulated in the GelMA gels (In-GelMA) versus cells that escaped the hydrogel (Escaped). B) Percentage of LSK, GMP, and PMN cells in suspension or GelMA (Escaped + In-GelMA cells) after 7 days. D) Percentage of LSK, GMP, and PMN cells in suspension, in-GelMA, and escaped after 7 days of differentiation culture. E) Median Fluorescence Intensity (MFI) of LysM-EGP+ cells after 7 days of differentiation culture. N = 3 for all experiments. Suspension data points are represented with a dot symbol and white bars, GelMA with a square symbol and light grey bars, and Escaped with a triangle symbol and dark grey bars. * Denotes significance ($p < 0.05$) in comparison to the rest of the groups; ** ($p < 0.01$).

suspension (Figure 4C). Thus, PMN expanded from HSPC in GelMA and those isolated from bone marrow exhibited a greater capacity to degranulate and upregulate membrane CD11b receptors in response to ionophore-mediated calcium flux.

To further examine the antimicrobial functions of PMNs differentiated in GelMA, neutrophil extracellular trap (NET) formation and phagocytosis of *S. aureus* were measured (**Figure 5A**). PMNs cultured in GelMA showed equivalent levels of NETosis following exposure to the gram-negative bacteria *Pseudomonas aeruginosa* compared with bone marrow isolated cells (Figure 5B). In contrast, PMNs expanded in suspension and scored a higher baseline level, but generated a smaller increase in NETosis compared to bone marrow or GelMA. We next tested the capacity for phagocytosis of the gram-positive bacteria *S. aureus* coated bioparticles. PMNs expanded in GelMA gels or suspension registered increased phagocytic capacity compared with those extracted from the bone marrow (Figure 5C). Taken together, phenotypic analysis of effector functions indicates that HSPC expansion in GelMA or suspension produces more mature PMN with a greater capacity for antibacterial activation than those from bone marrow.

2.4. GelMA Hydrogels Provide a Synthetic Niche for Neutrophil Transplantation

After characterizing the survival, expansion, and activation potential of PMNs derived from HSPCs encapsulated in GelMA gels, we assessed the potential of 5% GelMA as a 3D niche for the delivery of HSPCs and expanded PMNs in vivo. HSPCs extracted from MRP8-FFLUC mice, which possess firefly luciferase (FFLUC) inserted in the myeloid-related protein 8 (MRP8) promoter region, were used to image and quantify PMN expansion. We first confirmed that the MRP8-FFLUC luciferase signal correlated directly with PMN numbers (Figure S4, Supporting Information). We quantified myeloid differentiation and expansion of PMNs from HSPCs encapsulated in 5% GelMA hydrogels compared with those maintained in suspension culture in either

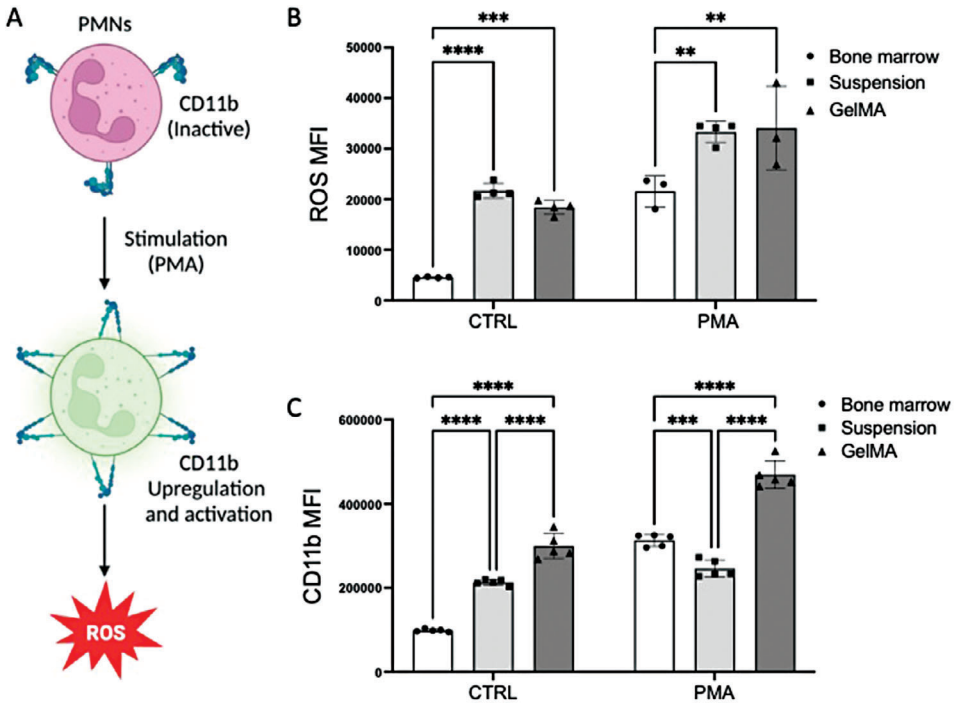

Figure 4. Analysis of ROS production and CD11b expression in neutrophils expanded from HSPCs encapsulated in GelMA compared to suspension-grown and bone marrow isolated. A) Schematic showing inactivated neutrophils responding to PMA and subsequently upregulating and activating CD11b and increasing ROS production. B) Reactive Oxygen Species (ROS) Median Fluorescence Intensity (MFI) of CD11b+ neutrophils extracted from bone marrow (C57BL/6J mice) or cultured in vitro for 7 days in either suspension or GelMA, when exposed to no stimulus (CTRL) or to 10 ng mL^{-1} of PMA. C) CD11b MFI in CD11b+/LysM+ neutrophils extracted from the bone marrow (LysM-EGFP mice) or cultured in vitro for 7 days in either suspension or GelMA, N = 3–5 for both experiments. Bone marrow data points are represented with a dot symbol and white bars, Suspension with a square symbol and light grey bars, and GelMA with a triangle symbol and dark grey bars. ** Denotes significance ($p < 0.01$), *** ($p < 0.001$), and **** ($p < 0.0001$).

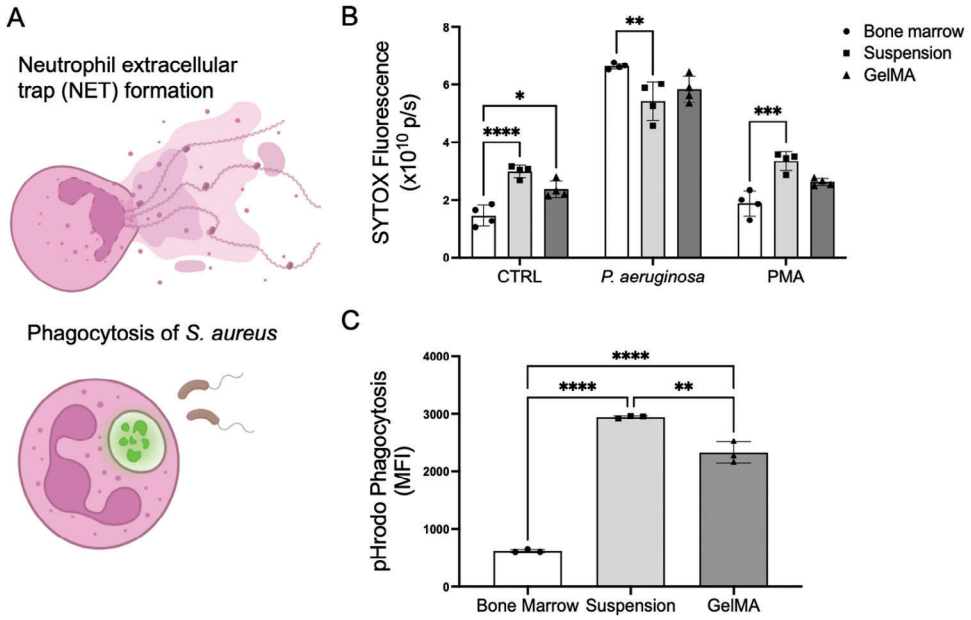

Figure 5. Analysis of neutrophil function in response to bacterial infection. A) Schematic defining the biological responses measured in this figure. B) Average fluorescence of SYTOX Orange as an analog for NETosis. C) Average fluorescence pH-reactive *S. aureus* bioparticles phagocytosed by EGFP+ cells and measured via AttuneNxT flow cytometer. Cells in both experiments were seeded and expanded for 7 days. N = 3–4. * Denotes significance ($p < 0.05$), ** ($p < 0.01$), *** ($p < 0.001$), and **** ($p < 0.0001$).

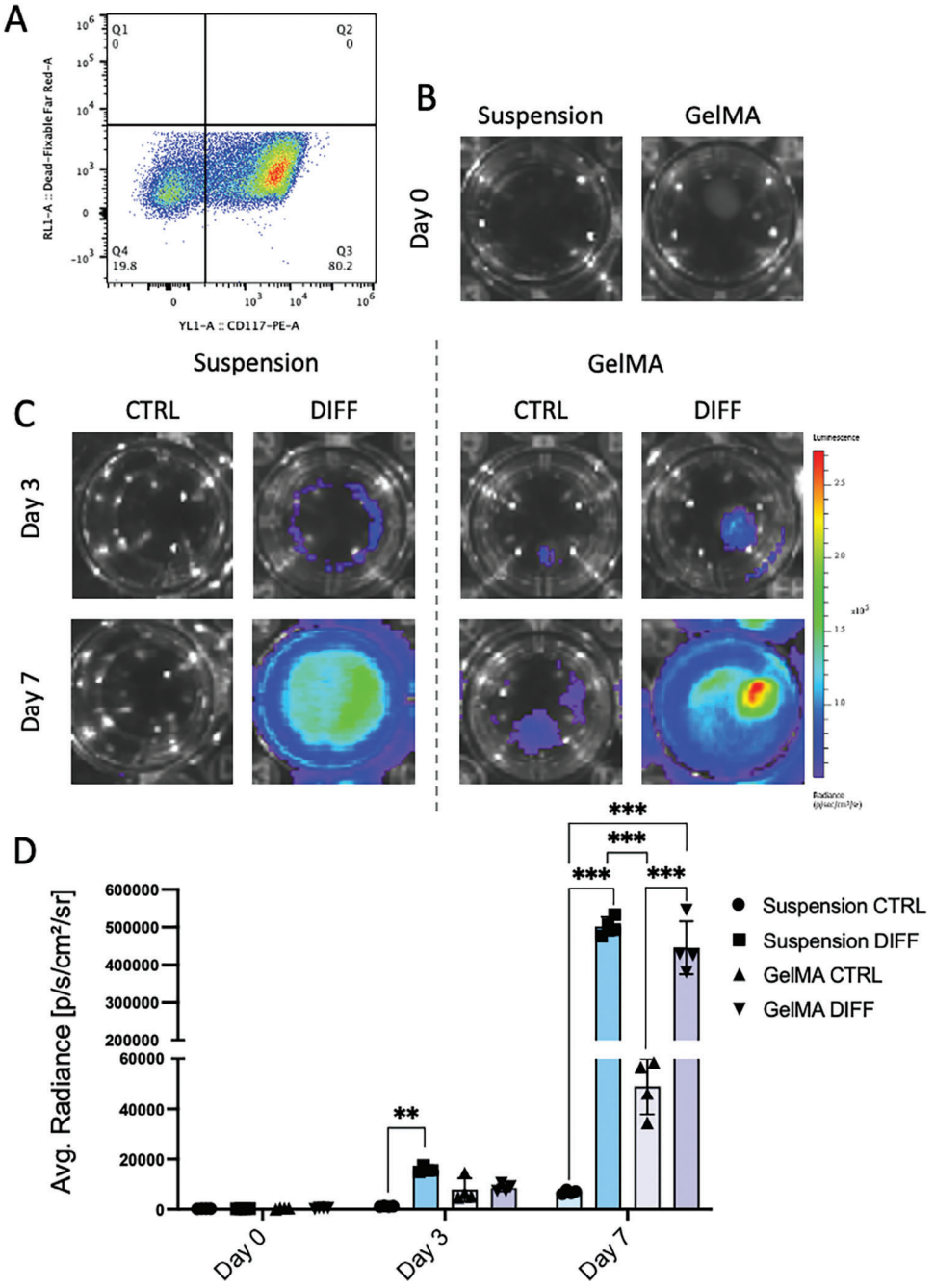

Figure 6. Luciferase activity of MRP8-FFLUC HSPCs cultured in vitro in either suspension or encapsulated in 5% GelMA hydrogels. A) Confirmation of >80% of CD117$^+$ HSPCs after cell isolation from the bone marrow of MRP8-FFLUC mice. B) Luciferase activity at day 0 after isolation in cells in suspension or encapsulated in 5% GelMA gels. C) Luciferase activity after 3 and 7 days of in vitro culture in cells cultured in suspension or encapsulated in GelMA gels and maintained in basal (CTRL) or differentiation (DIFF) media. D) Quantification of luciferase activity (N = 4). Suspension CTRL data points are represented with a dot symbol and light blue bars, Suspension Diff with a square symbol and darker blue, GelMA CTRL with a triangle and light purple bars, and GelMA Diff with an inverted triangle and darker purple bars. ** Denotes significance ($p < 0.01$) and *** ($p < 0.001$).

non-supplemented basal media (CTRL) or differentiation (DIFF) media. After HSPC isolation, luciferase activity indicative of mature PMNs was not observed in HSPCs seeded either in suspension or 5% GelMA hydrogels (**Figure** 6A,B), confirming that naïve HSPCs do not express the FFLUC gene product. Following 3 days of in vitro culture, luciferase activity was present in cells in suspension and those encapsulated in GelMA gels cultured in DIFF media, revealing the capacity to initiate granulopoiesis (Figure 6C,D). After 7 days of culture, luciferase activity levels between the suspension and the GelMA groups cultured in DIFF media were not significantly different, but GelMA typically exhibited focal sites of higher expansion activity. In contrast, when

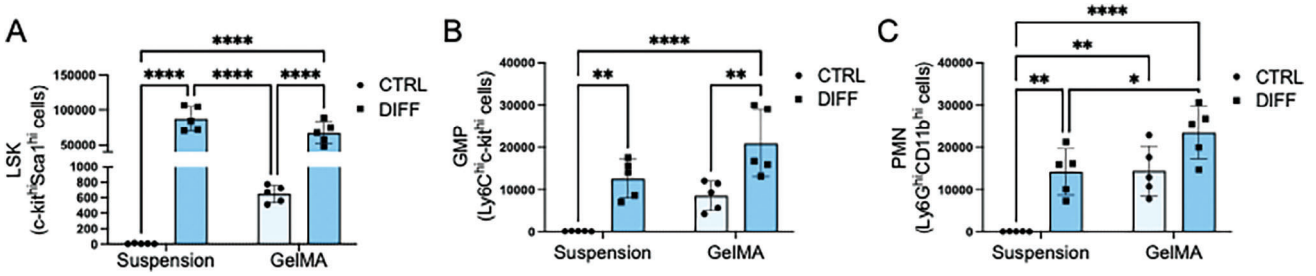

Figure 7. Phenotypic characterization of MRP8-FFLUC cell populations cultured in suspension or GelMA in maintenance (CTRL) or differentiation (DIFF) media. (A-C) Number of LSK (Sca-1$^+$c-kit$^+$), GMP (Ly6C$^+$c-kit$^+$), and PMN (Ly6G$^+$CD11b$^+$) cells after 7 days of in vitro culture. N = 5 for all experiments. CTRL and DIFF data points are represented with dot symbols and clear blue bars and with square symbols and dark blue bars respectively. * Denotes significance ($p < 0.05$); ** ($p < 0.01$) and **** ($p < 0.0001$).

cultured in CTRL media, luciferase activity was only detected in the GelMA group (Figure 6C,D).

The cell populations cultured in suspension or GelMA were analyzed by flow cytometry to assess the relationship between luciferase expression and HSPC differentiation. The quantity of LSK, GMP, and PMN cells was significantly higher in the suspension and GelMA groups cultured in differentiation media in comparison to culture in control media (**Figure** 7A–C). Consistent with the luciferase activity depicted in Figure 6, we detected a significantly higher expansion efficiency of PMNs in the GelMA group in comparison to the suspension group when cultured in control conditions. We conclude that GelMA hydrogel cultures produce greater numbers of mature PMNs versus suspension cultures even when the frequency of LSK and GMPs are present at similar numbers.

Finally, we explored the potential of GelMA hydrogels to serve as a synthetic niche for the transplantation of HSPC-derived PMNs in vivo. HSPCs isolated from MRP8-FFLUC mice were cultured either in suspension or encapsulated in 5% GelMA for 7 days in differentiation media conditions (**Figure** 8A). After confirming a similar level of luciferase activity (e.g., PMN and progenitor numbers) in the suspension and GelMA groups (Figure 8B), the cells in suspension or cell-laden gels were transplanted into the flank of C57BL/6J mice and luciferase activity was monitored for 5 days. Cells encapsulated in GelMA were able to survive following 5 days of implantation without loss of PMN phenotype as confirmed by luciferase activity (Figure 8C). Conversely, cells in suspension were less prevalent visually with a 40% reduction in signal detection at 5 days. Neutrophils in the GelMA gels also remained localized to the implanted area, highlighting the potential of this system to precisely control sites of granulopoiesis after transplantation (Figure 8C).

3. Discussion

We applied GelMA hydrogels as a synthetic 3D scaffold for encapsulation and maintenance of naïve HSPCs in 3D in vitro culture, as well as their ability to undergo granulopoiesis and expand into mature PMNs. Bone marrow-derived HSPCs from LysM-EGFP and MRP8-FFLUC reporter mice provided continuous readouts of the expansion efficiency and maturation of HSPCs into GMPs and PMNs. Encapsulated HSPCs exhibited 100% higher efficiency of LSK retention and granulocyte expansion and provided a means to concentrate PMN that retained the capacity to escape the hydrogel. These PMNs were functional based on their capacity to upregulate membrane CD11b, undergo stimulated ROS production, and produce NETs and phagocytose bacteria. Finally, we demonstrated that this approach allows for in vivo implantation of HSPC-loaded gels and detects site-specific granulopoiesis, which is clinically relevant for the local production of PMN at sites of acute and chronic infection.

Our design criteria were focused on engineering a 3D microenvironment that mimicked the fibrous nature and stiffness of the stem cell niche in the bone marrow. In this work, GelMA was chosen as a 3D matrix for HSPC cultivation due to its biocompatibility, tunable mechanical properties, the promotion of cell-substrate interactions, and degradability via cell-secreted enzymes. Previous reports revealed the storage modulus of bone marrow to be between 0.25 and 24.7 kPa, leading us to generate 5%, 10%, and 20% GelMA constructs with a range of stiffness from 0.2 to 10 kPa.[20] The 5% gels, with Young's modulus of ≈0.2 kPa, exhibited the highest maintenance of HSPC survival 24 h post-encapsulation. This stiffness and porosity correlated with increased DNA content, low activity of apoptotic markers, and increased cytoskeletal activity of HSPCs within the microenvironment. Maintaining the self-renewal properties of naïve LSK populations is crucial for the most efficient generation of GMPs that fuel granulopoiesis. Like previous reports that used 4% GelMA gels for the maintenance of LSK phenotype during in vitro culture, FACS analysis revealed that ≈10–20% of cells in gel cultures one week after encapsulation retained an LSK phenotype.[18] Confocal images after 7 days of culture also revealed CD117+ cells surrounded by numerous progenitors at various stages of differentiation evidenced by polymorphonuclear cells consistent with granulocyte development and EGFP+ reporter expression. Our goal in using a 3D crosslinked gelatin matrix was to provide a synthetic niche that maintains HSPC self-renewal and increases the quantity of GMPs and PMNs produced per input LSK compared to suspension cultures. Thus, we observed a ≈20-fold expansion of GMPs in GelMA versus a ≈15-fold expansion in suspension culture after 3 days, and a onefold increase in PMNs produced compared to suspension cultures. Previous studies expanding human CD34+ HSPCs in a suspension bioreactor required 7 days to reach a 20-fold expansion of GMPs versus 3 days in our GelMA cultures.[26] These results also confirm previous 3D collagen substrate studies reporting that suspension culture of HSPCs yields fewer differentiated GMPs and PMNs than 3D microenvironments.[17]

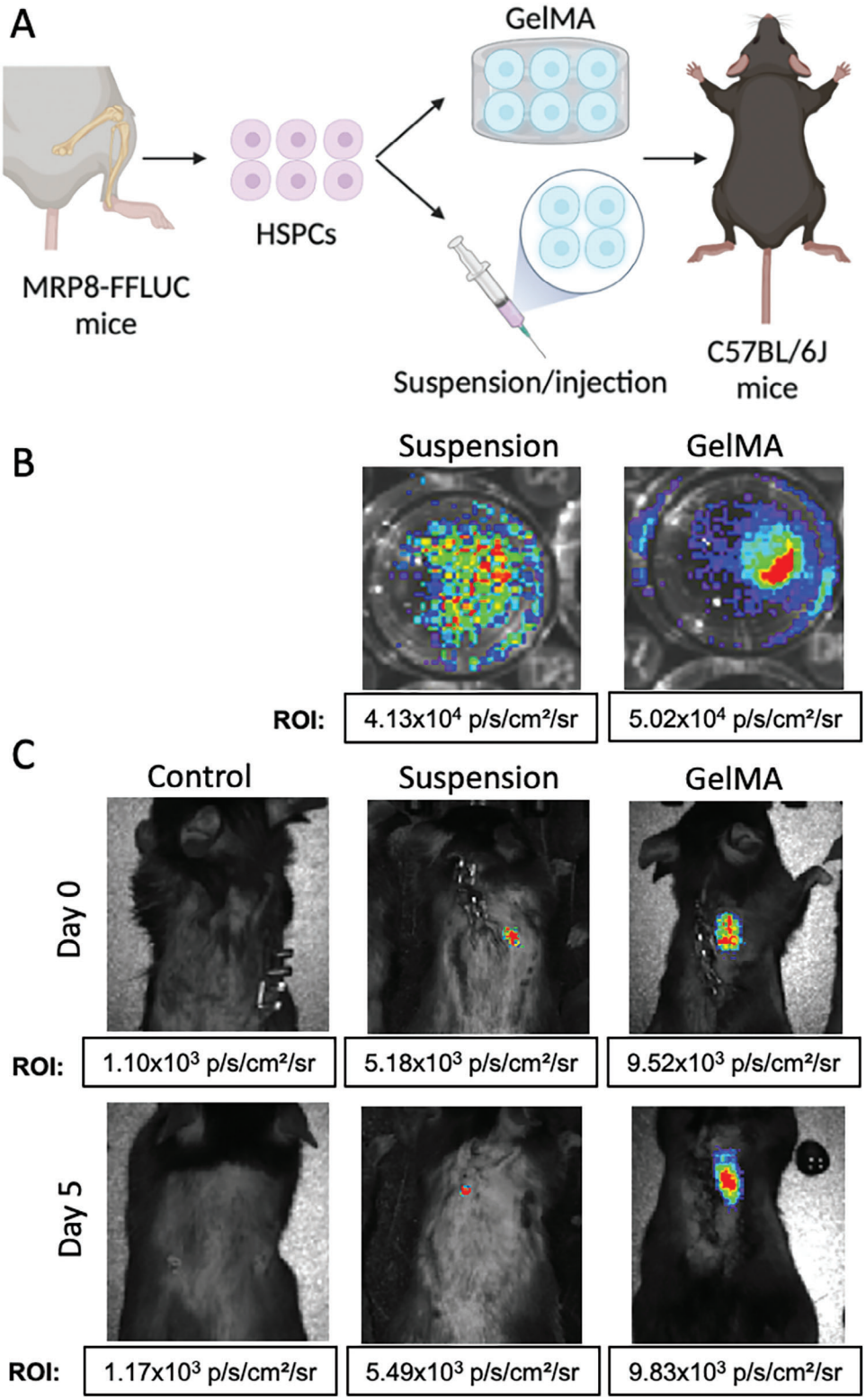

Figure 8. Transplantation of neutrophils expanded from MRP8-FFLUC HSPCs cultured in either suspension or GelMA gels into C57BL/6J mice. A) Schematic of the experimental flow. B) Luciferase activity in the suspension and GelMA groups after 7 days of in vitro culture. C) Luciferase activity of cells in suspension or GelMA at days 0 and 5 after transplantation into C57BL/6J mice.

HSPC differentiation and PMN maturation were visualized using HSPCs harvested from the femurs of LysM-EGFP reporter mice.[19] These reporter mice were previously used to demonstrate the phenomenon of extramedullary granulopoiesis in *S. aureus* infected wounds where they provided up to 20% of resident PMNs within 3 days.[13] The LysM-EGFP reporter was also useful in FACS studies to quantify HSPC differentiation to GMPs and PMNs. Utilizing this approach, we observed that LSK-seeded hydrogels showed improved differentiation into GMPs, whereby day 3 gels produced ≈8 PMNs per seeded HSPC compared to ≈3 PMNs in suspension cultures. Over time, however, the compared expansion efficiency at day 7 in in vitro cultures is less prominent than that at day 3. We believe this may relate to the limitation of nutrient availability and cell–cell contact inhibition that limits the rate of HSPC expansion at later time points. The total cell expansion rate in suspension and GelMA conditions remained similar, indicating that the matrix provided a milieu that promoted granulocyte differentiation in response to inflammatory cytokines and growth factors. Extracellular matrices affect transport through transient interactions of cytokines and growth factors with substrates that can hinder diffusion and advection.[27,28] With this in mind, encapsulated HSPCs and LSK progenitors in the GelMA may receive fewer signals from soluble media factors that direct differentiation (paracrine signaling), and increased cell–cell communication directed differentiation (autocrine signaling). Since PMNs secrete collagenase such as MMP14 that facilitates matrix remodeling, we investigated the phenotypic differences in cells that remained in and escaped the gels.[29] After one week of culture, ≈40% of the total cells escaped the gels, confirming the capacity of GMPs and PMNs to exit the GelMA matrix. LSK cells were predominantly found in the gel phase rather than escaping into the suspension. This observation may reflect the mechanism of PMN extravasation from human bone marrow, which continuously are recruited into the circulation while maintaining naïve HSPC populations. This is further evidenced by the observation of increased F-actin-mediated cytoskeletal activity and adhesion of HSPCs within the 5% GelMA. In future studies, we anticipate that this transport phenomenon could be leveraged to improve PMN expansion produced in bioreactors where GMPs and PMNs can be continually expelled from GelMA while LSK and early progenitors remain encapsulated in their niche to maintain granulopoiesis. This motivates future work involving bioreactor-based manufacturing of ex vivo neutrophils and the generation of mathematical models that can predict the transport of egressed cells leaving 3D matrices for optimization of the biomanufacturing process. GelMA cultures also generated PMNs expressing higher levels of lysozyme M, an antimicrobial effector molecule responsible for bacterial wall degradation, in EGFP+ cells compared to suspension conditions.[30] This leads us to believe that 3D culture conditions are more suited for greater phenotypic expression of lysozyme markers.

The oxidative burst capacity of neutrophils is a hallmark of the antimicrobial function of mature myeloid immune cells. After 7 days of GelMA culture, isolated CD11b+ cells responded to PMA stimulation of Protein Kinase-C by increasing ROS production to a greater degree than bone marrow cells. GelMA expanded PMN expressed higher baseline ROS than bone marrow PMN when unstimulated. This supports the contention that CD11b+ PMNs derived from HSPCs expanded in GelMA both match and exceed the antimicrobial functional capacity of bone marrow-derived PMN. CD11b is an important integrin on the surface of mature PMNs that mediates the transition from cell arrest to a migratory state capable of extravasation through inflamed endothelium.[16,25,31] A measure of PMN degranulation is the upregulation of CD11b via release from granule stores to the plasma membrane within minutes of chemotactic stimulation.[25] EGFP+CD11b+ GelMA PMNs were capable of >50% upregulation in CD11b expression rapidly after PMA stimulation, whereas suspension cells only registered a ≈10% increase. These results suggest that PMNs expanded in cytokine-supplemented suspension cultures have delayed maturation and lack the signaling machinery necessary for chemotactic stimulation, lowering their capacity as functional antimicrobial phagocytes.

Mature PMNs in the body generate nuclear extracellular traps (NETs) to ensnare bacteria in the wound environment. All cell cultures were able to generate NETs in response to *P. aeruginosa* stimulation, however, suspension-expanded PMNs demonstrated significantly less NETosis than bone marrow-isolated PMNs. These results further support the inferiority of suspension cultures to GelMA cultures in terms of antimicrobial capacity. Another important antimicrobial function of neutrophils is the ability to clear bacteria from an infected wound through phagocytosis. Here we note that GelMA EGFP+ cells phagocytosed somewhat fewer *S. aureus* coated bioparticles than those expanded in suspension. However, both suspension and GelMA cultures on average phagocytosed a significantly greater number of bioparticles than bone marrow cells. This confirms that PMN expanded in culture with growth factor, cytokine, and Flt3-ligand enriched media at baseline are more mature and capable of antibacterial functions.

Luciferase co-expressed with MRP8 as a mature neutrophil reporter allowed us to assess growth dynamics employing IVIS spectral imaging in real-time without disturbing the culture system. We expected to observe the radiance of these cultures increase with time in supplemented differentiation media. Unexpectedly, HSPCs in GelMA exhibited a strong FFLUC signal in the absence of differentiation factor supplementation, despite the absence of growth factors. This observation supports the hypothesis that GelMA constructs provide a more conducive 3D microenvironment that increases the survival of HSPCs via paracrine activity. This effect is likely attributed to the optimal physical properties of GelMA that facilitate cell-matrix and homotypic adhesion and remodeling. Because this phenomenon was consistently observed in GelMA and not suspension cultures, we conclude that the 3D growth environment can be optimized to promote HSPC renewal and expansion, implying the importance of the mechanical properties of the matrix that promote granulopoiesis.[18]

While suspension and GelMA cultures both exhibited comparable average radiance, the luminescence of GelMA cultures exhibited focal areas of PMN expansion, suggesting that granulopoiesis is promoted within the 3D construct. The limited field of view of confocal imaging limited the precise quantification of these areas of high cell density that support greater focal expansion of granulocytes. HSPC differentiation and expansion were confirmed by FACS analysis, revealing greater numbers of GMPs and PMNs produced in the GelMA matrix. The

enhanced capacity of MRP8-FFLUC HSPCs to undergo granulopoiesis in GelMA was demonstrated by transplanting them into full-thickness skin wounds of C57BL/6J mice. Suspension cultures quickly dispersed in wounds after implantation whereas gels retained a strong focal bioluminescent signal after 5 days. Earlier we addressed how the expansion of HSPC in GelMA may be limited in culture over time, unlike suspension cultures. However, for the use of adoptive transfer for local granulocyte expansion, encapsulating cells leads to more overall HSPCs in the wound environment. Previously, we have shown that early PMN expansion is critical for host survival against virulent *S. aureus*.[15] Future studies will focus on the delivery of HSPC-loaded GelMA gels directly to the site of a skin wound or infection in an immunodeficient mice model that requires PMN expansion for resolution.[15]

Despite the success of optimized PMN expansion within HSPC GelMA discs demonstrated here, several limitations should be noted. The elevated expression of CD11b observed in both suspension and GelMA cultures compared to bone marrow suggests that the media cocktail containing IL-3 and IL-6 may prematurely activate PMNs.[32,33] This may lead to desensitization of PMNs due to premature activation when eventually applied therapeutically.[34,35] Additionally, many safety concerns must be addressed before the implantation of GelMA constructs into the wounds of human patients. Difficulties surrounding successfully deploying this therapy include isolating a patient's own bone marrow cells, the time it takes to naturally degrade this gel in vivo, and the effects of delayed inflammation resolution.[36–38] A potential limitation of this system is that PMNs would need time to escape from their gel after maturation. However, PMNs are capable of migration in confined 3D spaces. Further, MMP14 expression was upregulated in cells encapsulated in GelMA compared to escaped cells, supporting our hypothesis that PMN can degrade the gels and exit into the wound space. When we compare GelMA therapy to injecting suspended HSPCs directly into the wound site, cells rapidly diffuse out. Therefore, we believe encapsulation of HSPCs will still lead to more neutrophils effectively in the wound site despite the time needed to escape. PMNs also produce other factors that assist in immune defense, such as NETs, enzymes, and reactive oxygen species that would diffuse out of the gel space and into the infection space.

4. Conclusion

This study focused on the optimization of a 3D GelMA hydrogel to mimic the bone marrow niche for HSPC encapsulation and enhanced PMN expansion. There is a need to address the challenge of ex vivo PMN expansion as a viable means of providing functional PMNs for neutropenic patients who undergo chemotherapy or immunodeficient patients requiring acute innate immunotherapy. By establishing a biomimetic bone marrow environment for HSPCs, we demonstrated the importance of an appropriate 3D microenvironment to support HSPC differentiation and PMN expansion while retaining phagocyte functionality. Furthermore, our findings elaborate on potential therapeutic applications, such as implanting encapsulated HSPCs at wound sites to boost innate immune function in acute infections in patients with neutropenia. Future work should concentrate on further optimization of the 3D substrate and evaluation of the full therapeutic potential of HSPC-seeded hydrogels in clinically relevant skin infection models such as antibiotic-resistant gram-negative and positive bacteria.

5. Experimental Section

Generation of Transgenic Mice and Ethical Approval: EGFP-lysozyme M (LysM) knock-in mice (EGFP-LysM-mice[19]) were kindly gifted by Dr. Thomas Graf(Center for Genomic Regulation, Spain). To generate the MRP8-FFLuc line, the following mouse strains were obtained from the Jackson Laboratories (Bar Harbor, Maine) and cross-bred at the University of California, Davis: B6.Cg-Tg(S100A8-cre,-EGFP)1Ilw/J (Jax Strain #02 1614)[39] and STOCK Gt(ROSA)26Sortm1(Luc)Kael/J (Jax Strain #03 4320).[40] To identify and select offspring mice expressing the firefly luciferase reporter, mice were subcutaneously administered 250 mg kg^{-1} of D-Luciferin (Cat#: 122 799, Perkin Elmer, Waltham, Massachusetts) and imaged in an IVIS Spectrum (Perkin Elmer, Waltham, Massachusetts)[41]. All animal experiments were approved by the Institutional Animal Care and Use Committee (IACUC) of the University of California at Davis and were performed following the guidelines of the Animal Welfare Act and the Health Research Extension Act.

HSPC Isolation and In Vitro Culture: Murine bone marrow cells were harvested from the hind legs of 8-week-or-older EGFP-LysM knock-in mice. After euthanasia with CO2, femurs, fibulas, and tibias were aseptically collected, ground in EasySep Buffer, (STEMCELL Cat#: 20 144), and filtered through a 70 µm strainer. Cells were negatively isolated using the EasySep Mouse Hematopoietic Progenitor Cell Isolation Kit (STEMCELL Cat #19856A) and then isolated and selected using the EasySep Mouse CD117 (cKIT) Positive Selection Kit (STEMCELL Cat#: 18 757). Cells were resuspended at 1E6 cells mL^{-1} in HSPC expansion media, containing STEMSPAN SFEM II (STEMCELL), recombinant murine stem cell factor (0.1 µg mL^{-1}, SCF, STEMCELL), recombinant murine Flt3-ligand (0.1 µg mL^{-1}, STEMCELL), recombinant murine granulocyte colony-stimulating factor (0.01 µg mL^{-1}, G-CSF, STEMCELL), recombinant murine interleukin 3 (0.01 µg mL^{-1}, IL-3, STEMCELL), and recombinant murine interleukin 6 (0.01 µg mL^{-1}, IL-6, STEMCELL).

HSPCs were cultured in 48-well suspension culture plates with 1 mL of HSPC expansion media per well. Each well received 2×10^5 HSPCs in suspension or encapsulated in GelMA, incubated at 37 °C, 5% CO_2, and fed every 2 days.

GelMA Gel Production and Mechanical Properties Characterization: GelMA gels were produced as previously described.[42] Briefly, Gelatin methacryloyl (GelMA; 300 bloom, MilliporeSigma, St. Louis, MO) was dissolved at 20% (w/v) in complete media with 0.6% (w/v) 2-Hydroxy-4′-(2-hydroxyethoxy)−2-methylpropiophenone (Irgacure 2959) with agitation at 80 °C for 15 min. The 20% GelMA was then diluted in complete media to yield a 5% GelMA or 10% GelMA solution containing 0.3% Irgacure. HSPCs were encapsulated in the different GelMA solutions to a final concentration of 5E6 cells mL^{-1}. The final solution was dispensed (40 µL) into 6 mm diameter × 1 mm high molds and exposed to 17 mW cm^{-2} ultraviolet (UV, 320–500 nm) light for 1 min before culture using an OmniCure S2000 Spot UV Curing System (Excelitas Technologies, Waltham, MA).

The mechanical and physical properties of the GelMA gels were analyzed as previously described.[43] The storage modulus of 8 mm diameter × 2 mm height gels was analyzed using a Discovery HR-2 hybrid stress-controlled rheometer. The constructs were placed between 8 mm parallel plates (axial force set at 0.2 N) and were strained from a range of 0.001–5% with a frequency of 1 Hz. The values of storage modulus (G') were obtained from the linear viscoelastic region. Volumetric swelling ratio (Q) was calculated by the following equation as previously described:

$$Q = \frac{\frac{W_S - W_D}{\rho_W} + \frac{W_D}{\rho_P}}{\frac{W_D}{\rho_P}} \quad (1)$$

where ρ_W is the density of water and ρ_P is the density of the polymer (1.35 g mL^{-1}).[43,44] Mesh size of the crosslinked polymers in the constructs was estimated using swelling and storage modulus as previously described.[43–45] The molecular weight between crosslinks (M_C) was then determined via the following equation:

$$M_C = C_P\, RT/G' \tag{2}$$

where C_P is the polymer concentration, R is the gas constant, and T is the temperature. Mesh size (ξ) was then calculated as follows:

$$\xi = Q^{\frac{1}{3}}\, l\left(\frac{2M_C}{M_r}\right)^{\frac{1}{2}} C_n^{\frac{1}{2}} \tag{3}$$

Where the molecular weight of the repeating unit M_r (91.19 g mol^{-1}), the amino acid bond length l (4.28 Å), and Flory's characteristic ratio C_n for GelMA (8.8785) as previously described.[45]

To obtain the hydrogel swelling ratio, the wet weight (WS) of the constructs was recorded, the constructs were frozen at −80 °C overnight, lyophilized for 48 h, and then weighed again to obtain the dry weight (WD).

HSPC Viability and Morphology Assessment: For visualization of cell morphology, cell-laden GelMA constructs were collected after 1 day of culture and fixed with 4% paraformaldehyde at 4 °C overnight, washed twice with PBS, and permeabilized with Triton-X 100 (0.05%) for 5 min at room temperature. Cell actin cytoskeleton was stained with Alexa Fluor 488 Phalloidin solution (Thermo Fisher; 1:40 in PBS). Cell nuclei were stained with DAPI (Thermo Fisher; 1:500 in PBS). Gels were imaged using confocal microscopy (Leica TCS SP8). Cell viability was analyzed by a live/dead assay (LIVE/DEAD Viability/Cytotoxicity Kit) per the manufacturer's protocol (Thermo Fisher) in which samples are simultaneously stained with green-fluorescent calcein-AM to indicate intracellular esterase activity and red-fluorescent ethidium homodimer-1 to indicate loss of plasma membrane integrity. Fluorescent images were taken using confocal microscopy (Leica TCS SP8, Wetzlar, Germany). The percentage of living cells and cell shape descriptors were quantified through image analysis in ImageJ. For quantification of DNA level and caspase 3/7 activity, constructs were collected, sonicated, and lysed in a passive lysis buffer (Promega, Madison, WI). Total DNA content was determined using a PicoGreen Quant-iT PicoGreen DNA Assay Kit (Invitrogen). Cell apoptosis was measured using a Caspase-Glo 3/7 assay (Promega, Madison, WI). For both assays, a BioTek Synergy HTX Multi-mode Microplate Reader (Agilent).

RT-qPCR: Samples were collected in 0.3 mL of TRIzol Reagent (Invitrogen) and homogenized using an ultrasonic processor. RNA was isolated following the manufacturer's instructions. Following RNA isolation, 800 ng of RNA was reverse-transcribed with the QuantiTect Reverse Transcription Kit (QIAGEN) and normalized to a final concentration of 12 ng µL^{-1}. RT-qPCR was performed using the Taqman PCR Master Mix (QIAGEN) on a QuantStudio 6 system (Applied Biosystems). Mice-specific primers for *GAPDH* (Mm99999915_g1), *MMP14* (Mm00485054_m1), and *MMP8* (Mm00439509_m1) were purchased from ThermoFisher Scientific. Critical threshold values (Ct) were quantified for each gene. The ΔCt was quantified by subtracting the samples' Ct value of the housekeeping gene, *GAPDH*. The ΔΔCt was quantified by subtracting the average ΔCt of the suspension cells on Day 7. The relative expression values for each gene of interest are presented at $2^{-\Delta\Delta Ct}$.

GelMA Culture Confocal Imaging: Gels were cultured for 7 days before being fixed in Fixation Buffer (Biolegend) for 1 h. Gels were then incubated in 5 µg mL^{-1} DAPI for 30 min before being washed twice and imaged on an Olympus FV3000 confocal microscope with a 60x objective. The EasySep Mouse CD117 (cKIT) Positive Selection Kit (STEMCELL Cat#: 18 757) that was used on day 0 to isolate HSPCs contains a PE-CD117 antibody used in the isolation process, and this antibody conjugate persisted over 7 days and the fixation process and is seen in confocal images.

HSPC Phenotypic Characterization: Cell-laden gels were cultured for 7 days before being collected individually. Hydrogels were fragmented using a scalpel and incubated in collagenase type IV (1000 Units mL^{-1}, Gibco) at 37 °C for 20 min. Escaped and suspension cells were harvested by gently pipetting and transferring to a new tube. This process was repeated with EasySep Buffer to detach over 90% of cells. After centrifugation and washing with EasySep Buffer, cells were labeled with a panel of antibodies for 30 min: CD117-PE (Biolegend Cat#: 105 808, 1:100), CD11b-Alexa Fluor 700 (Biolegend Cat#: 101 222, 1:1000), SCA-1-APC (Biolegend Cat#: 108 112, 1:1000), Ly6C-APC/Fire750 (Biolegend Cat#: 128 046, 1:100), Ly6G-PE/Cy7 (Biolegend Cat#: 127 618, 1:100), and fixable viability dye eFluor506 (Thermo Fisher Cat#: 65-0866-14, 1:1000). Flow cytometry was performed using the Attune NxT Acoustic Focusing Flow Cytometer (Thermo Fisher). Compensation controls, unstained samples, and fluorescence minus one control were used to gate cell populations (See Figures S5 and S6, Supporting Information).

CD11b Upregulation Assay: Cells were isolated as described earlier, with encapsulated and escaped cells combined from hydrogel wells. Cells from three GelMA wells were pooled and divided into three tubes for stimulation. This process was serially repeated, using 15 wells for N = 5 replicates. Suspension cells were similarly pooled. After centrifugation, cells were resuspended in HBSS +/+ and 0.1% human serum albumin containing PMA (10 ng mL^{-1}). Cells were labeled with CD11b-Brilliant Violet 711 (Biolegend Cat#: 101 242, 1:1000), and Zombie Yellow Fixable Viability dye (Biolegend Cat#: 423 103, 1:100). Tubes were incubated for 20 min at 37 °C, followed by treatment with Fixation Buffer (Biolegend). Cells were washed with EasySep Buffer twice before flow cytometry was performed using the Attune NxT Acoustic Focusing Flow Cytometer (Thermo Fisher).

ROS Activity: Cells were isolated with encapsulated and escaped cells combined from hydrogel wells. After centrifugation, cells were resuspended in tubes with HBSS +/+ and placed on a 37 °C hotplate to warm for 45 min. Depending on condition, tubes were treated with 10 ng/mL PMA and labeled with CD11b-Brilliant Violet 711 (Biolegend Cat#: 101 242, 1:1000), Dihydrorhodamine 123 (Thermo Fisher Cat#: D23806, 10 µM), and Zombie Yellow Fixable Viability dye (Biolegend Cat#: 423 103, 1:1000). Tubes were incubated at 37 °C for another 20 min before the reaction was extinguished by placing on ice for 10 min. Cells were spun down and resuspended in EasySep buffer and measured using the Attune NxT Acoustic Focusing Flow Cytometer (Thermo Fisher).

NETosis Assay: Cells from individual 9 cultures were isolated at day 7 and pooled. 1E5 cells mL^{-1} were seeded into a 96 well plate in HBSS +/+ in the presence of *P. aeruginosa* (1E8 CFU), PMA, or vehicle control. Plates were then incubated for 12 h at 37 °C stained with 20 µL of 5 µM SYTOX Orange and incubated a room temperature for 15 min. Plates were then imaged on the IVIS Spectrum for SYTOX orange to measure NET output.

Phagocytosis Assay: N = 3 cultures of cells were isolated at a density of 1E6 cells mL^{-1} for each condition of GelMA, suspension, or bone marrow cells. Phagocytosis was induced using a pHrodo *S. aureus* BioParticle Phagocytosis kit using the kit's protocol. pHrodo MFI was measured on EGFP+ cells using an AttuneNxT flow cytometer.

Luciferase Activity Quantification and In Vivo Cell Transplantation: On day 7, hydrogel constructs with encapsulated PMN derived from HSPC of MRP8-FFLuc mice were sub-dermally implanted into recipient C57Bl6/J mice. >20 min prior to surgery, mice intraperitoneally received 0.03 mg mL^{-1} Buprenex. Dorsal area of each mouse was shaven and aseptically sterilized with gauze in povidone-iodine and gauze in 70% isopropanol. An intradermal pouch was created using surgical scissors into which hydrogel constructs were transplanted. The pouch was stitched and mice were monitored for recovery. Mice received a daily subcutaneous dose of 250 mg kg^{-1} of D-Luciferin 5 min prior to imaging in an IVIS Spectrum to quantify MRP8-luciferase activity in vivo. As a proof of concept of therapeutic application, a sample size of N = 1 was used in this experiment for each of the groups. All animal experiments were approved by the Institutional Animal Care and Use Committee (IACUC) of the University of California at Davis and were performed following the guidelines of the Animal Welfare Act and the Health Research Extension Act.

Statistical Analysis: Data are presented as means ± standard deviation unless otherwise stated and all data points are included in each graph. Normality was tested through the Shapiro–Wilk test ($\alpha = 0.05$). Statistical analysis was done using one-way ANOVA with post-hoc Tukey test, two-way ANOVA with Tukey's multiple comparisons test, or unpaired *t*-test when necessary. For data following a non-normal distribution,

Kruskal–Wallis test was used. $p < 0.05$ was considered significant. Statistical significance was indicated in each graph as * ($p < 0.05$), ** ($p < 0.01$), *** ($p < 0.001$), and **** ($p < 0.0001$).

Ethics Approval Statement: Animal studies were approved by the Institutional Animal Care and Use Committee (IACUC) at the University of California, Davis under protocol codes 19922 and 21790.

Supporting Information

Supporting Information is available from the Wiley Online Library or from the author.

Acknowledgements

T.G.-F. would like to acknowledge the support received through start-up funds by Lehigh University. E.P.C. and S.I.S. would like to acknowledge Megan Westerland for her assistance in conducting experimental methods. E.W. would like to acknowledge the support from the California Institute of Regenerative Medicine grant number ECUC4-12792 (CIRM EDUC4 Research Training Program). The authors would also like to acknowledge Kevin P. Francis, Ph.D., at the University of California Los Angeles David Geffen School of Medicine for his assistance in designing the MRP8-FFLuc mouse line and optimizing the quantitative luciferase assays. This work was funded by NIH AI129302 to S.I.S. and J.K.L. and EB030410 to S.I.S. T.G.-F. would like to acknowledge start-up funds provided by the Department of Bioengineering and the P.C. Rossin College of Engineering & Applied Science at Lehigh University.

Conflict of Interest

The authors declare no conflict of interest.

Data Availability Statement

The data that support the findings of this study are available from the corresponding author upon reasonable request.

Keywords

extramedullary granulopoiesis, gelatin methacrylate (GelMA), hematopoietic stem and progenitor cells (HSPCs), neutrophils

Received: June 21, 2023
Revised: February 7, 2024
Published online: February 25, 2024

[1] L. Mölne, M. Verdrengh, A. Tarkowski, *Infect. Immun.* **2000**, *68*, 6162.
[2] M. Verdrengh, A. Tarkowski, *Infect. Immun.* **1997**, *65*, 2517.
[3] H. Hirai, P. Zhang, T. Dayaram, C. J. Hetherington, S. Mizuno, J. Imanishi, K. Akashi, D. G. Tenen, *Nat. Immunol.* **2006**, *7*, 732.
[4] W. M. Nauseef, N. Borregaard, *Nat. Immunol.* **2014**, *15*, 602.
[5] S. Hämäläinen, T. Kuittinen, I. Matinlauri, T. Nousiainen, I. Koivula, E. Jantunen, *Leuk Lymphoma* **2008**, *49*, 495.
[6] L. Sung, R. Aplenc, T. A. Alonzo, R. B. Gerbing, T. Lehrnbecher, A. S. Gamis, *Blood* **2013**, *121*, 3573.
[7] A. A. Marfin, T. H. Price, *J. Intensive Care Med.* **2015**, *30*, 79.
[8] M. A. Torres-Acosta, R. P. Harrison, E. Csaszar, M. Rito-Palomares, M. E. G. Brunck, *Front. Med.* **2019**, *6*.
[9] E. A. Silva, E.-S. Kim, H. J. Kong, D. J. Mooney, *Proc. Natl. Acad. Sci. USA* **2008**, *105*, 14347.
[10] E. Sleep, B. D. Cosgrove, M. T. McClendon, A. T. Preslar, C. H. Chen, M. H. Sangji, C. M. R. Pérez, R. D. Haynes, T. J. Meade, H. M. Blau, S. I. Stupp, *Proc. Natl. Acad. Sci. USA* **2017**, *114*, E7919.
[11] K. C. Rustad, V. W. Wong, M. Sorkin, J. P. Glotzbach, M. R. Major, J. Rajadas, M. T. Longaker, G. C. Gurtner, *Biomaterials* **2012**, *33*, 80.
[12] T. Gonzalez-Fernandez, P. Sikorski, J. K. Leach, *Acta Biomater.* **2019**, *96*, 20.
[13] M.-H. Kim, J. L. Granick, C. Kwok, N. J. Walker, D. L. Borjesson, F.-R. E. Curry, L. S. Miller, S. I. Simon, *Blood* **2011**, *117*, 3343.
[14] J. L. Granick, P. C. Falahee, D. Dahmubed, D. L. Borjesson, L. S. Miller, S. I. Simon, *Blood* **2013**, *122*, 1770.
[15] P. C. Falahee, L. S. Anderson, M. B. Reynolds, M. Pirir, B. E. McLaughlin, C. A. Dillen, A. L. Cheung, L. S. Miller, S. I. Simon, *J. Immunol.* **2017**, *199*, 1772.
[16] E. Kolaczkowska, P. Kubes, *Nat. Rev. Immunol.* **2013**, *13*, 159.
[17] B. P. Mahadik, N. A. K. Bharadwaj, R. H. Ewoldt, B. A. C. Harley, *Biomaterials* **2017**, *125*, 54.
[18] A. E. Gilchrist, S. Lee, Y. Hu, B. A. C. Harley, *Adv. Healthcare Mater.* **2019**, *8*, 1900751.
[19] N. Faust, F. Varas, L. M. Kelly, S. Heck, T. Graf, *Blood* **2000**, *96*, 719.
[20] L. E. Jansen, N. P. Birch, J. D. Schiffman, A. J. Crosby, S. R. Peyton, *J. Mech. Behav. Biomed. Mater.* **2015**, *50*, 299.
[21] L. S. Anderson, M. B. Reynolds, K. R. Rivara, L. S. Miller, S. I. Simon, *J. Vis. Exp.* **2019**, https://doi.org/10.3791/59015.
[22] W. C. Parks, C. L. Wilson, Y. S. López-Boado, *Nat. Rev. Immunol.* **2004**, *4*, 617.
[23] M. Wysoczynski, R. Reca, H. Lee, W. Wu, J. Ratajczak, M. Z. Ratajczak, *Leukemia* **2009**, *23*, 1455.
[24] C. C. Winterbourn, A. J. Kettle, M. B. Hampton, *Annu. Rev. Biochem.* **2016**, *85*, 765.
[25] N. Dixit, S. I. Simon, *Front. Immunol.* **2012**, *3*.
[26] N. E. Timmins, E. Palfreyman, F. Marturana, S. Dietmair, S. Luikenga, G. Lopez, Y. L. Fung, R. Minchinton, L. K. Nielsen, *Biotechnol. Bioeng.* **2009**, *104*, 832.
[27] A. Pluen, P. A. Netti, R. K. Jain, D. A. Berk, *Biophys. J.* **1999**, *77*, 542.
[28] C. C. van Donkelaar, G. Chao, D. L. Bader, C. W. J. Oomens, *Comput. Methods Biomech. Biomed. Engin.* **2011**, *14*, 425.
[29] K. A. Hasty, M. S. Hibbs, A. H. Kang, C. L. Mainardi, *J. Biol. Chem.* **1986**, *261*, 5645.
[30] P. Markart, T. R. Korfhagen, T. E. Weaver, H. T. Akinbi, *Am. J. Respir. Crit. Care Med.* **2004**, *169*, 454.
[31] A. Cappenberg, M. Kardell, A. Zarbock, *Cells* **2022**, *11*, 1310.
[32] G. F. Weber, B. G. Chousterman, S. He, A. M. Fenn, M. Nairz, A. Anzai, T. Brenner, F. Uhle, Y. Iwamoto, C. S. Robbins, L. Noiret, S. L. Maier, T. Zönnchen, N. N. Rahbari, S. Schölch, A. K.-V. Ameln, T. Chavakis, J. Weitz, S. Hofer, M. A. Weigand, M. Nahrendorf, R. Weissleder, F. K. Swirski, *Science* **2015**, *347*, 1260.
[33] L. Borish, R. Rosenbaum, L. Albury, S. Clark, *Cell. Immunol.* **1989**, *121*, 280.
[34] K. Kienle, K. M. Glaser, S. Eickhoff, M. Mihlan, K. Knöpper, E. Reátegui, M. W. Epple, M. Gunzer, R. Baumeister, T. K. Tarrant, R. N. Germain, D. Irimia, W. Kastenmüller, T. Lämmermann, *Science* **2021**, *372*, eabe7729.
[35] H. Ali, R. M. Richardson, B. Haribabu, R. Snyderman, *J. Biol. Chem.* **1999**, *274*, 6027.
[36] N. Pineault, A. Abu-Khader, *Exp. Hematol.* **2015**, *43*, 498.
[37] S. Heltmann-Meyer, D. Steiner, C. Müller, D. Schneidereit, O. Friedrich, S. Salehi, F. B. Engel, A. Arkudas, R. E. Horch, *Biomed. Mater.* **2021**, *16*, 065004.
[38] B. E. Sansbury, M. Spite, *Circ. Res.* **2016**, *119*, 113.
[39] M.-H. Kim, W. Liu, D. Borjesson, F. Curry, L. Miller, A. Cheung, F.-T. Liu, R. Isseroff, S. Simon, *J. Invest. Dermatol.* **2008**, *128*, 1812.

[40] M. Safran, W. Y. Kim, A. L. Kung, J. W. Horner, R. A. DePinho, W. G. Kealin, *Mol. Imaging* **2003**, *2*, 297.
[41] G. Wang, C. Zhang, H. Kambara, C. Dambrot, X. Xie, L. Zhao, R. Xu, A. Oneglia, F. Liu, H. R. Luo, *Front Immunol* **2022**, *13*, 875991.
[42] R. C. H. Gresham, D. Kumar, J. Copp, M. A. Lee, J. K. Leach, *Tissue Eng., Part C* **2022**, *28*, 239.
[43] T. Gonzalez-Fernandez, A. J. Tenorio, K. T. Campbell, E. A. Silva, J. K. Leach, *Tissue Eng., Part A* **2021**, *27*, 1168.
[44] K. T. Campbell, R. S. Stilhano, E. A. Silva, *Biomaterials* **2018**, *179*, 109.
[45] M. Vigata, C. D. O'Connell, S. Cometta, D. W. Hutmacher, C. Meinert, N. Bock, *Polymers* **2021**, *13*, 3960.